

Journal of Biomedical Optics

BiomedicalOptics.SPIEDigitalLibrary.org

Concurrent photoacoustic-ultrasound imaging using single-laser pulses

Shi-Yao Hung
Wen-Shao Wu
Bao-Yu Hsieh
Pai-Chi Li

Concurrent photoacoustic-ultrasound imaging using single-laser pulses

Shi-Yao Hung,^a Wen-Shao Wu,^a Bao-Yu Hsieh,^a and Pai-Chi Li^{a,b,*}

^aNational Taiwan University, Graduate Institute of Biomedical Electronics and Bioinformatics, No. 1, Sec. 4, Roosevelt Road, Taipei 106, Taiwan

^bNational Taiwan University, Department of Electrical Engineering, No. 1, Sec. 4, Roosevelt Road, Taipei 106, Taiwan

Abstract. Conventional ultrasound (US) and photoacoustic (PA) multimodality imaging require the use of a US pulse for US data acquisition and a laser pulse for PA data acquisition. We propose a method for concurrent US and PA data acquisition with a single-laser pulse. A light-absorbing multilayer film that can generate a US pulse based on the thermoelastic effect is used. The selection of appropriate layer thickness, interlayer spacing, and absorption coefficient allows the spectral characteristics of the generated US signal to be adjusted so that it does not overlap with the spectrum of the PA signal generated by the light transmitting through the layer. Thus, the US signal and the PA signal can be generated, received, and separated by using a single-laser pulse combined with spectral filtering. This method is demonstrated using a multilayer film that generates US signals with a center frequency of 24.2 MHz and fractional bandwidth of 26.8%. The synthetic-aperture focusing technique is applied to improve the lateral resolution and the signal-to-noise ratio. A cyst-like phantom and a film phantom were used to demonstrate the feasibility of this method of concurrent PA-US imaging using single-laser pulses. © 2015 Society of Photo-Optical Instrumentation Engineers (SPIE) [DOI: 10.1117/1.JBO.20.8.086004]

Keywords: photoacoustic imaging; laser-generated ultrasound; multimodality imaging.

Paper 150275R received Apr. 27, 2015; accepted for publication Jul. 9, 2015; published online Aug. 11, 2015.

1 Introduction

Photoacoustic (PA) imaging involves forming an image based on optical contrast with resolution characteristics consistent with those of ultrasound (US). In contrast, US imaging is based on acoustic backscattering, and is typically used to provide structural information with penetration better than that of PA imaging. Both US and PA imaging have received widespread research interest due to their applications in dermatology,¹ ophthalmology,² intravascular imaging,³ and small-animal imaging.⁴ Because US imaging and PA imaging are complementary to each other and share the same receiver hardware, it is natural to combine these two modalities into a single system. Multimodality imaging is typically implemented using a laser for PA imaging and a US transmitter. The laser pulse and the US pulse are fired sequentially, and the received US signals are used to form the PA image and the US image, respectively. Although this approach is straightforward, it requires separate transmission hardware and the two images may be misaligned in the presence of motion.

The goal of this study was to develop a concurrent imaging approach using only a single-laser pulse to acquire both PA and US image data. In this approach, the laser pulse impinges on a multilayer film, with part of the laser energy absorbed by the film and the rest passing through it. The film is designed so that the absorbed light energy induces a thermoelastic effect, and the subsequently generated US is used for US imaging, while the laser energy transmitting through the film is used for PA imaging. These two types of signals are received by the same transducer. Certain parameters associated with the multilayer structure of the light-absorbing film, including the layer thickness, interlayer

spacing, and absorption coefficient, are optimized to reduce the spectral overlap between the two signals. This allows a simple spectral filter to be used to separate the PA signal from the US signal, hence, only single-laser pulses are needed for concurrent PA and US data acquisition.

The thin-film approach was already proposed in the literature for optical generation of US as an alternative to the piezoelectric effect. It is based on the thermoelastic effect resulting from the absorption of laser energy, in which the thin film absorbs impinging laser energy, which leads to thermal expansion that generates a US wave. The optical generation of US has the advantages of high frequency and small element size, which is defined by the size and location of the focused laser beam. Light-absorbing thin films made from a mixture of carbon black and polydimethylsiloxane (PDMS), chromium,⁵ gold nanostructures,⁶ and carbon nanotube composite^{7,8} have been used to generate high-frequency (>50 MHz) and high-magnitude (~50 MPa)⁷ US.

In a previous study,⁹ we designed a US-PA dual-modality imaging system using a dichroic filter to switch between the following two imaging modes: (1) laser irradiation at the first wavelength was absorbed by the dichroic filter to generate the US waves for US imaging, while (2) laser pulses at the second wavelength passed through the filter and were used for PA imaging. In the different approach adopted in the present study, the two signals needed for US and PA imaging are separated in the frequency domain. The main hypothesis underlying this new approach is that a high-frequency narrowband US can be optically generated by using a multilayer light-absorbing film for US imaging and can be separated from low-frequency PA signals by simple spectral filtering (Fig. 1). The multilayer

*Address all correspondence to: Pai-Chi Li, E-mail: paichi@ntu.edu.tw

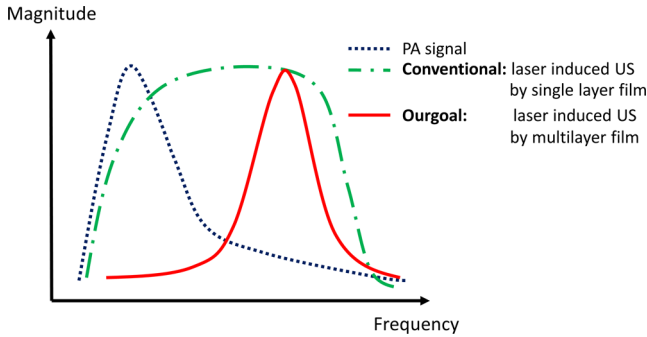


Fig. 1 Schematic of the single-pulse scheme.

light-absorbing film was designed to allow changes to the frequency spectrum of the generated US. The multilayer structure comprises multiple light-absorbing layers and multiple light-transmittance layers. The frequency of the generated US can be adjusted by tuning the optical absorption coefficient of the light-absorbing layers and by changing the thickness of the light-transmittance layers.

The absorption coefficients of biological tissues vary over a wide range, from 2.3 to 40 cm^{-1} , depending on the tissue type and laser wavelength. On the other hand, we have previously reported that the main frequency range (e.g., up to the -6 dB cutoff) of the PA signals generated by biological tissue is typically below 10 MHz ,¹⁰ which, in principle, can be separated from the high-frequency US ($>20 \text{ MHz}$) generated by the multilayer film. Considering the fact that the typical penetration depth for PA imaging of biological tissues is around 1 to 2 cm , the ideal frequency range for US imaging is around 20 to 40 MHz . Therefore, when the US signal is above 20 MHz , good contrast

between PA imaging and US imaging can be expected. In this regard, the main limitation of the proposed approach is the ability to generate a high-frequency and narrow band US signal from the multilayer film. In practice, it can be achieved only by having precise control of the absorbing coefficient, absorbance uniformity, and thickness of each absorbing layer, as well as the distance between adjacent layers. The feasibility of the proposed design is demonstrated herein by presenting the imaging results for two distinct types of phantom.

2 Materials and Methods

2.1 Multilayer Thin Film for Photoacoustic Generation of High-Frequency Narrowband Ultrasound

High-frequency broadband US signals can be generated by a single-layer thin film irradiated with laser pulses. The spectrum of the generated US signal generally has a broadband nature and thus overlaps with the spectrum of tissue PA signals, whose main components are typically below 10 MHz .¹⁰ To reduce the overlap and thereby enhance the contrast between the US and PA signals, it is necessary to generate narrowband acoustic signals. To achieve this goal, we propose using a multilayer structure instead of the conventional single-layer film. In principle, the US generated optically by a multilayer film can be expressed by the following equation

$$S_m(t) = S_s(t) * \sum_{i=1}^{2N-1} \alpha_i \delta(t - \tau_i) \triangleq S_s(t) * h_m(t), \quad (1)$$

where $S_m(t)$ represents the received PA signal generated by the multilayer film, $S_s(t)$ represents the PA signal generated by a

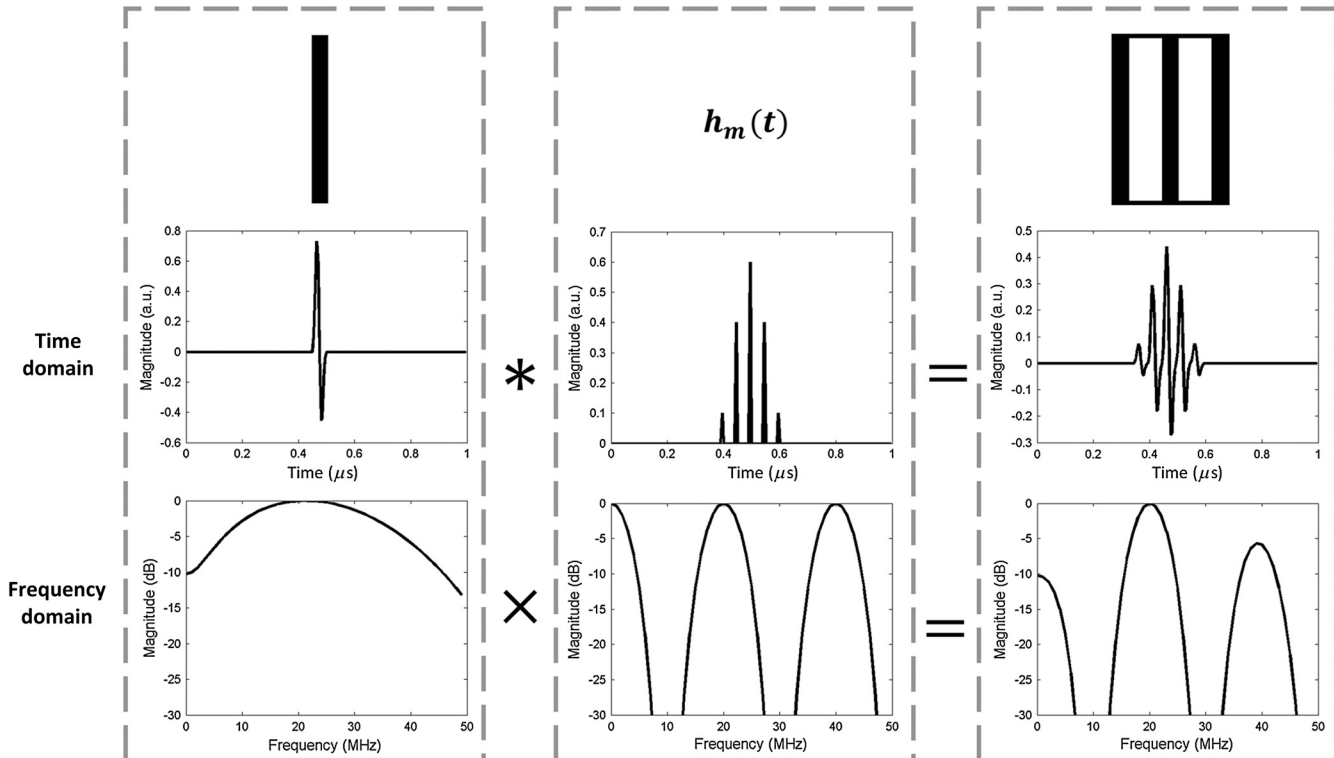


Fig. 2 Schematics of the generation process of the US signals and their spectra for a single-layer film and a multilayer film.

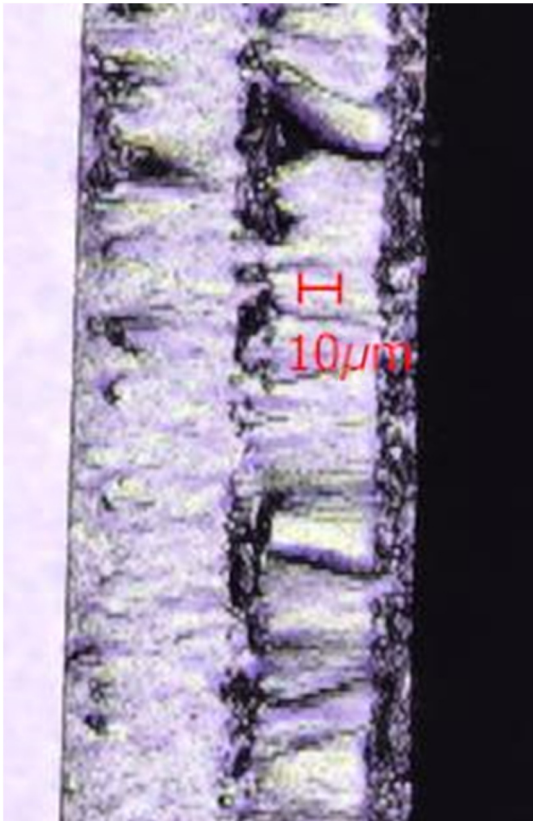


Fig. 3 Cross-sectional micrograph of a multilayer film.

single-layer film, N represents the number of light-absorbing layers, α_i is a constant corresponding to the optical absorption coefficient of each light-absorbing layer and the laser absorbance energy, τ_i is the time delay corresponding to the time of flight of the US propagating through the thickness of each light-transmittance layer, $h_m(t)$ represents the transfer function of the multilayer film, and $*$ is the convolution operator. Equation (1) indicates that the PA signal generated by the multilayer film can be considered as a superposition of $(2N - 1)$ single-film PA signals with different time delays and magnitudes, where the first N signals are generated directly by light-absorbing layers and the following $N - 1$ signals are the signals reflected from the glass substrate. Schematics of the generation process of the US signals and the corresponding spectra for a single-layer film and a multilayer film are shown in Fig. 2. The US signal generated by the multilayer film can be regarded as the US signal generated by a single-layer film convolved with a pulse train, and the frequency response of the US signal generated by the multilayer film is equivalent to the frequency response of the US signal generated by a single-layer film multiplied by the frequency response of the pulse train.

In one of our designs, the multilayer structure comprises three light-absorbing layers formed from a mixture of carbon black and PDMS, and two light-transmittance layers formed from pure PDMS. In this design, the carbon black was added as an optical absorber for converting the laser energy to the US based on the thermoelastic effect. To fabricate the multilayer film, the graphite-polymer mixture was first uniformly spin-coated onto a glass substrate at 6000 rpm for 45 s and then cured at 65°C for 1 h. Pure PDMS was then uniformly spin-coated onto the substrate to the appropriate thickness and

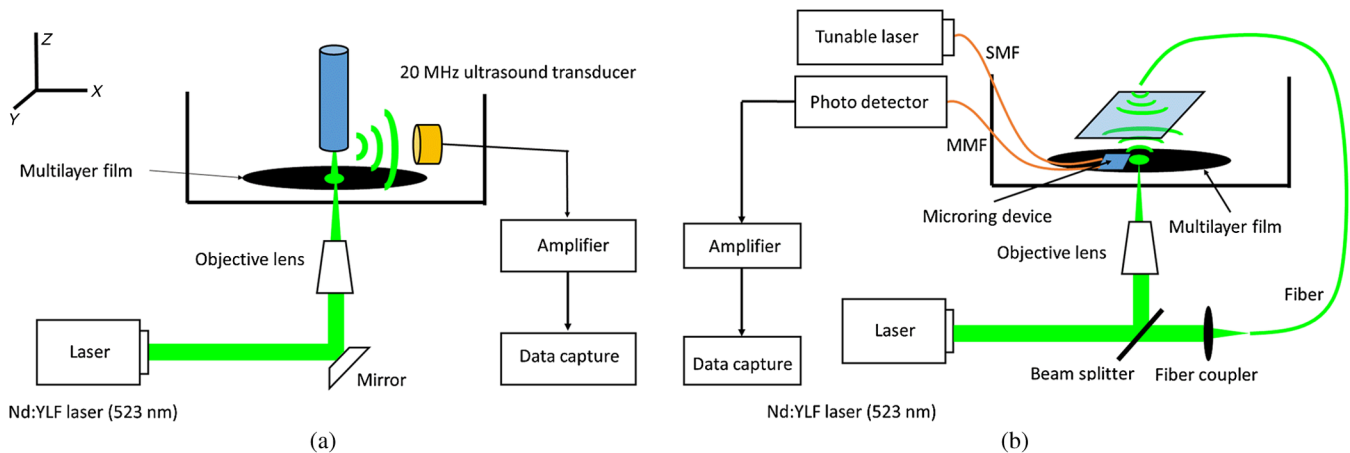


Fig. 4 (a) An integrated concurrent ultrasound-photoacoustic (US-PA) imaging system with a piezoelectric transducer and (b) an all-optical concurrent US-PA imaging system.

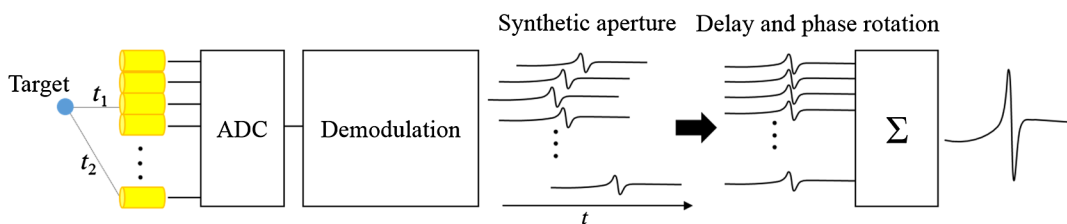


Fig. 5 Schematic of synthetic-aperture focusing technique (SAFT) signal processing.

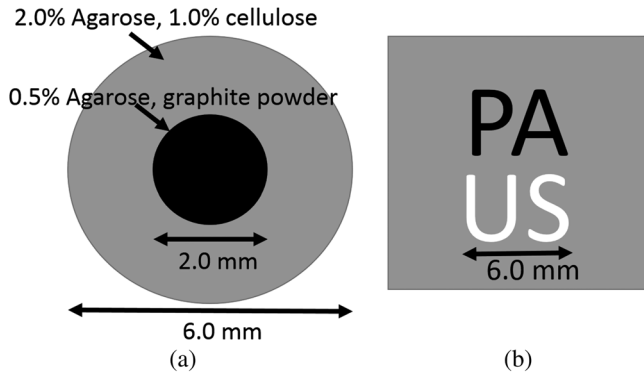


Fig. 6 Configurations of the (a) cyst-like phantom and (b) thin-film phantom.

cured. This process was repeated layer by layer in order to fabricate a multilayer film.

The signal magnitude from each layer can be tuned by adjusting the optical absorption coefficient of its corresponding light-absorbing layer, while the delay of each pulse can be adjusted by changing the thickness of its light-transmittance layer. Adjusting

these two parameters allows changes to both the center frequency and fraction bandwidth of the generated US: in principle, a thinner light-transmittance layer will result in the generation of a US signal with a higher-center frequency and broader bandwidth. Figure 3 shows a cross-sectional micrograph of a multilayer film consisting of three light-absorbing layers (each 10- μm thick) and two light-transmittance layers (each 30- μm thick).

2.2 Concurrent Ultrasound-Photoacoustic Imaging Scheme using Single-Laser Pulses

Two experimental setups of the concurrent US-PA imaging scheme are shown in Fig. 4. A diode-pumped Nd:YLF Q-switched pulsed laser (523 nm wavelength, 6 ns pulse width; IS8II-E, INNOSLAB Edgewave, Germany) is used for excitation. A pulse repetition rate of up to 5 kHz is possible with the Nd:YLF laser. To generate both US and PA signals with a single-laser pulse, the laser beam is focused on the multilayer film by an objective lens. The laser energy that is absorbed by the multilayer film becomes a US source, while the transmitting laser pulse irradiates the imaged object for PA imaging. In the first experimental configuration shown in Fig. 4(a), both the

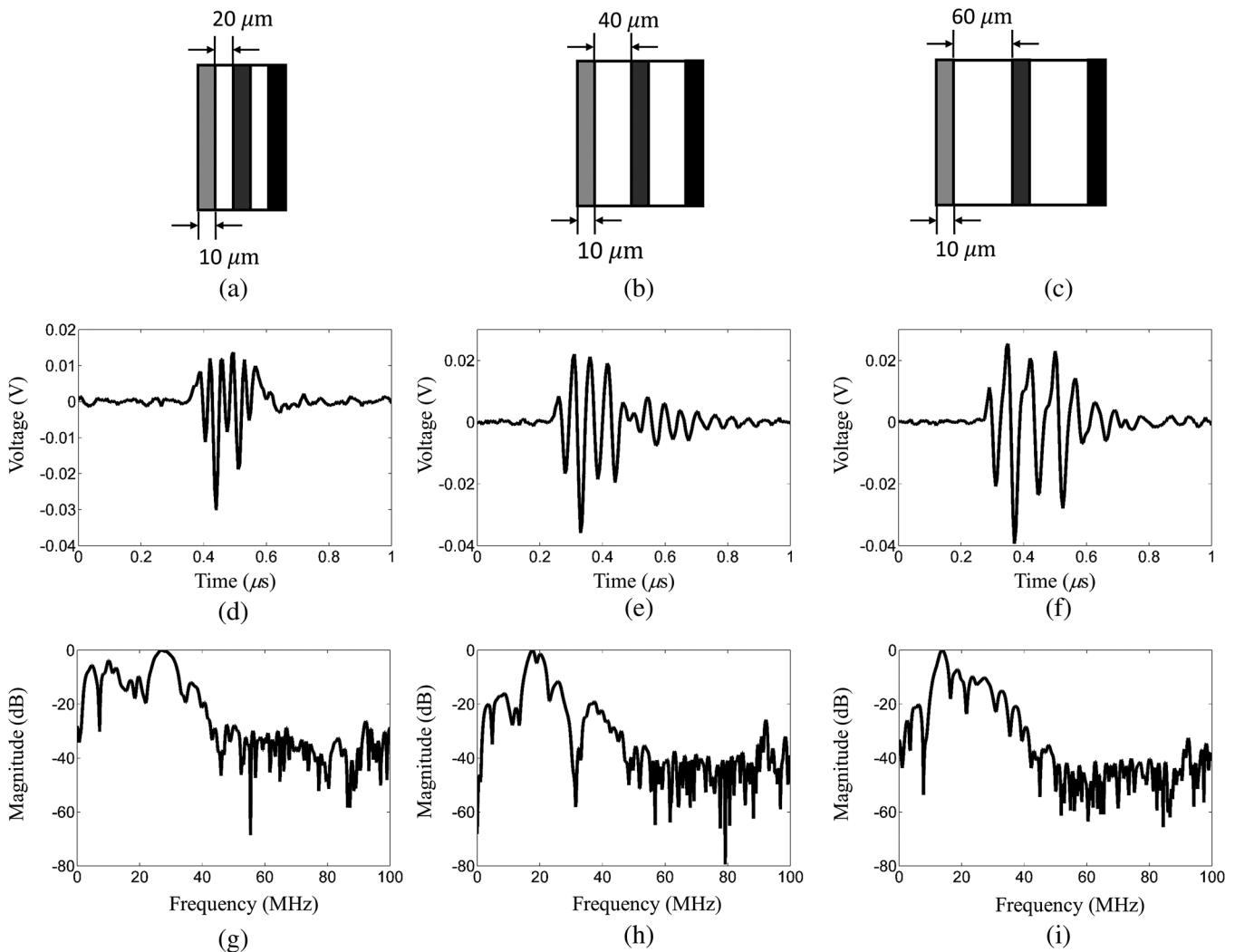


Fig. 7 (a)–(c) Multilayer structures comprising light-transmittance layers with different thicknesses, and the resulting (d)–(f) waveforms and (g)–(i) spectra.

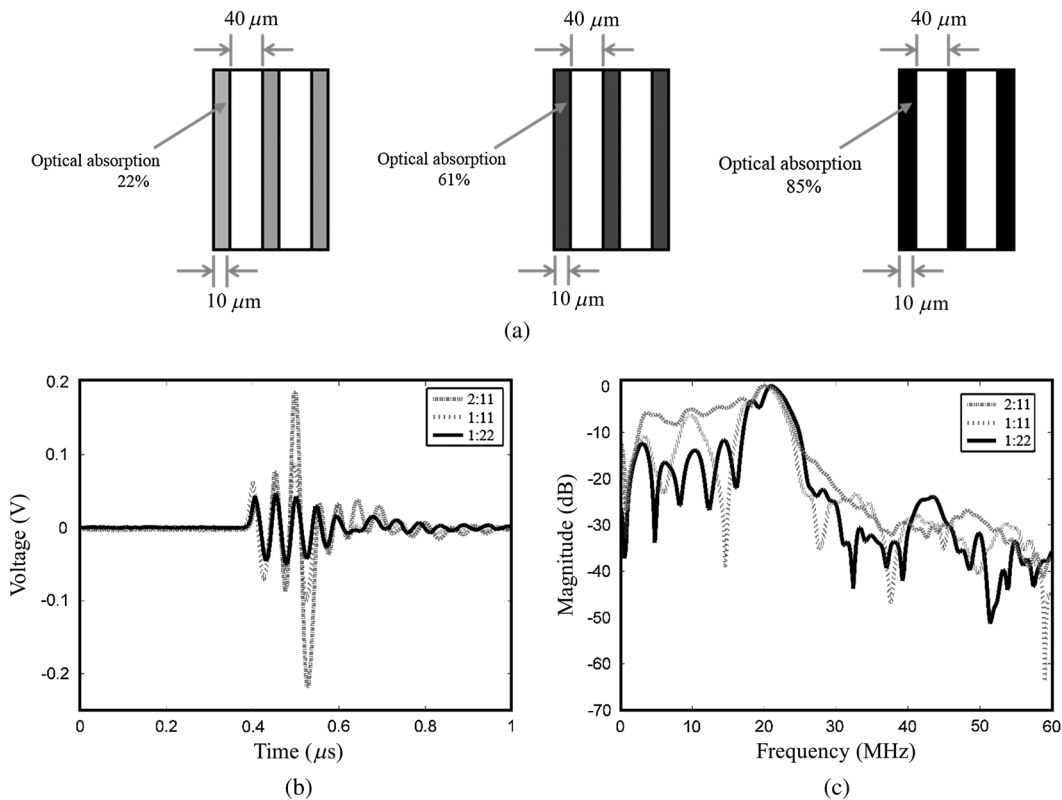


Fig. 8 (a) Multilayer structures comprising light-absorbing layers with different optical absorption coefficients, and the resulting (b) waveforms and (c) spectra. The keys in the graphs indicate the weight ratios of graphite concentration to polydimethylsiloxane.

Table 1 Variation of the center frequency of a multilayer structure with the interlayer spacing.

Interlayer spacing	20 μm	40 μm	60 μm
Center frequency (MHz)	27.8	18.5	13.8

US and PA signals from the imaged object are received by a 20-MHz homemade lithium niobate (LiNbO_3) US transducer. The mechanical scanning is performed with a precision motor (Z-108, Thorlabs, Newton, New Jersey) controlled by a personal computer to obtain B-mode images; a step size of 20 μm

produces 500 A-lines in a B-mode image. The detected US and PA signals are received and amplified by a pulser/receiver (5073PR, Olympus, Japan) and digitized by a 200 Msamples/s ADC (CompuScope 14200, Gage, Lachine, QC, Canada). A cyst-like phantom was used to test this setup.

The second experimental configuration is an all-optical-based US and PA dual-modality imaging system. A polymer microring resonator is used as the US detector. In the configuration shown in Fig. 4(b), the laser beam is split to generate both US and PA signals. One beam is focused on the multilayer film by the objective lens as a US source, and the other beam is coupled to a 550- μm multimode optical fiber (Thorlabs) by an optical lens to irradiate the imaged object for PA imaging. The US and PA signals are received by the polymer microring

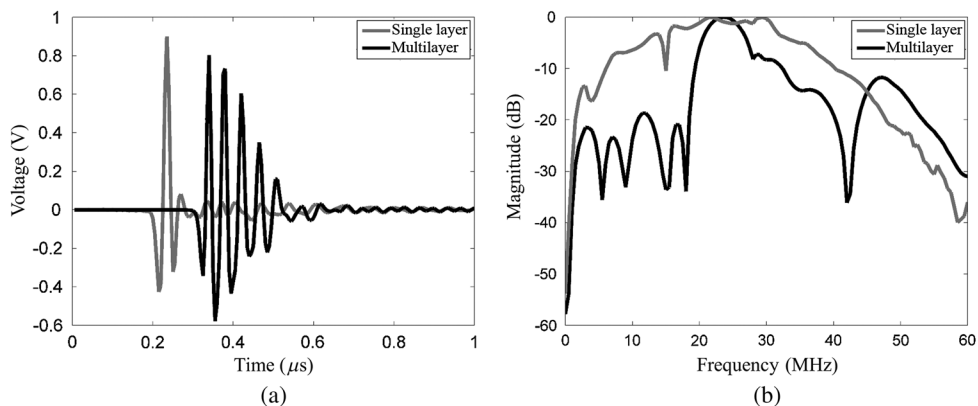


Fig. 9 (a) Waveforms and (b) spectra of US signals generated by a single-layer film and a multilayer film.

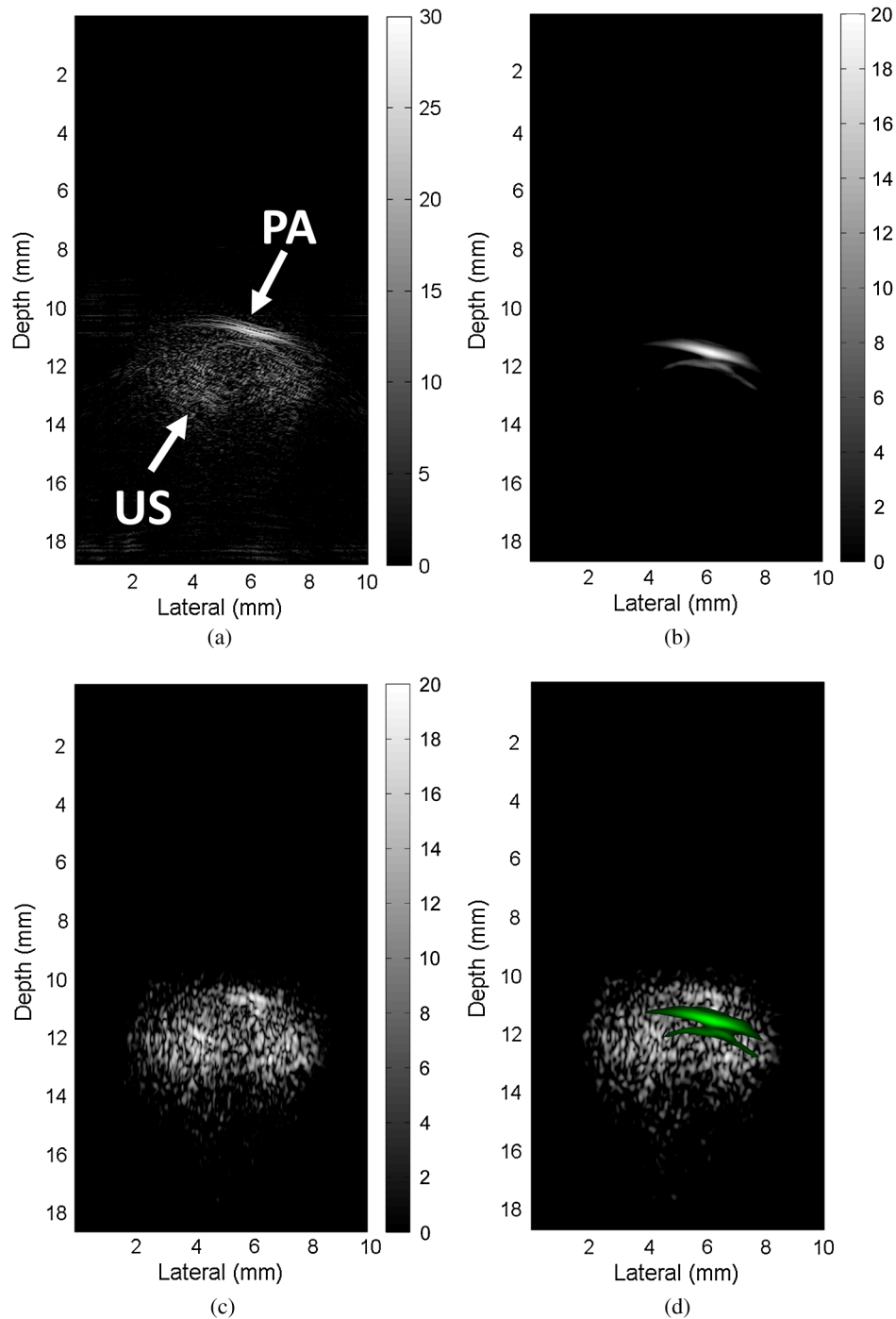


Fig. 10 (a) Original image with a single-laser pulse, (b) PA, (c) US enhanced image after SAFT algorithm, and (d) fusion image of the cyst-like phantom.

resonator, which is an optical-based US sensor. The microring resonator consists of a $100\text{-}\mu\text{m}$ diameter polystyrene ring waveguide that is closely coupled to a bent-back bus waveguide; this was fabricated by nanoimprint lithography. The input fiber is connected to another continuous-wave tunable laser (TSL-510, Santec, Aichi, Japan), and the output fiber is connected to a high-speed photodetector (1811-FC, New Focus, San Jose, California) with a gain of 4×10^4 V/A and an electrical bandwidth of 0 to 125 MHz. The acoustic pressure waveforms of backscattered US and PA signals can be recovered from the optical intensity at a specific wavelength.^{11,12}

The radiofrequency signals are digitized by a high-speed ADC at a sampling rate of 200 Msamples/s and then processed with two filters. The US signals are obtained using a 15 to 25 MHz bandpass filter and then demodulated at a center frequency of 20 MHz to baseband. The PA image data can be obtained by a 10-MHz lowpass filter and demodulated at a center frequency of 5 MHz. The baseband data from different laser scanning positions can be used to synthesize a larger array. The receive beam is formed by a synthetic-aperture focusing technique (SAFT)¹³ using the procedure shown in Fig. 5. This is implemented in the time domain using standard delay-and-sum

operations for receive focusing. For one-dimensional SAFT, the signals are delayed to a prespecified reference point and subsequently summed coherently. Finally, the processed US and PA images are fused to produce an image.

The performance characteristics of the two configurations were evaluated by imaging a cyst-like phantom and a thin-film phantom. A cyst-like phantom containing a single inclusion as shown in Fig. 6(a) was constructed using 2% agarose (0710, Amresco, Solon, Ohio) mixed with 1% cellulose, which served as acoustic scatterers. The cyst was constructed from 0.5% agarose mixed with graphite powder (282863, Sigma-Aldrich, St. Louis, Missouri), which has a particle size less than 20 μm and a high-optical absorption. The phantom and its cystic inclusion had diameters of 6.0 and 2.0 mm, respectively. The phantom was scanned by the concurrent US-PA imaging system [Fig. 4(a)] at a step size of 20 μm to prevent grating lobes appearing in the images. Each US and PA A-line signal was averaged 20 times to increase the signal-to-noise ratio (SNR).

The thin-film phantom comprised a carbon-black “PA” pattern printed on a thin plastic film and a “US” pattern carved by laser engraving with a line width of 1 mm and a letter size of 6 mm [Fig. 6(b)]. The thin-film phantom was scanned with the C-scan format to acquire US and PA three-dimensional information by the all-optical concurrent US-PA imaging system [Fig. 4(b)]. Each US and PA A-line signal was averaged 500 times to increase the SNR.

3 Results and Discussion

3.1 Multilayer Thin Film for Photoacoustic Generation of High-Frequency Narrowband Ultrasound

To demonstrate that the spectra of the recorded signals can be adjusted, two groups of multilayer structure were tested: (1) those comprising light-absorbing layers with the same optical absorption coefficient and light-transmittance layers with different thicknesses (20, 40, and 60 μm) (Fig. 7), and (2) those comprising light-transmittance layers with the same thickness and light-absorbing layers with different optical absorption coefficients (Fig. 8). The weight ratios of the graphite concentration to PDMS were 1:22, 1:11, and 2:11, which resulted in light absorptions of 22%, 61%, and 85%, respectively. An objective lens (BMO10, Qiset, Taiwan) was utilized to focus the laser beam onto the multilayer films, and a hydrophone (MHA9-150, Force Technology, Denmark) was used to record the generated US and PA signal, whose center frequency and bandwidth were measured.

Figure 7 illustrates the corresponding waveforms and their spectra generated by three multilayer structures; the center frequencies are listed in Table 1. The multilayer structure comprised three light-absorbing layers, and the optical absorption coefficient increased in the different individual light-absorbing layers when the peaks were normalized to the same magnitude, which means a wider signal envelope and a narrower bandwidth. The thickness of the single light-transmittance layer shown in Fig. 7(a) was 20 μm , and the speed of sound in PDMS is 1000 m/s,¹⁴ which means a theoretical delay of 20 ns per layer; this is consistent with the obtained experimental results. The corresponding waveforms and spectra of different multilayer films are shown in Fig. 4. The center frequency decreased from 27.8 to 13.8 MHz as the thickness of the light-transmittance layer increased from 20 to 60 μm , which also matches

the theoretical expectation. These experimental results demonstrate that using a thinner light-transmittance layer will increase the center frequency of the generated US.

Figure 8 shows different waveforms [Fig. 8(b)] and their corresponding spectra [Fig. 8(c)] generated by three different multilayer structures with different optical absorption coefficients [Fig. 8(a)]. The results show that the magnitude can be tuned by adjusting the optical absorption coefficient of the light-absorbing layers. A higher-optical absorption coefficient resulted in a higher-signal magnitude, narrower signal envelope, and broader bandwidth.

3.2 Concurrent Ultrasound-Photoacoustic Imaging Scheme Using Single-Laser Pulses

The subsequent imaging experiments used multilayer films with three 10- μm thick light-absorbing layers and two 35- μm thick light-transmittance layers. A weight ratio of the graphite concentration to PDMS of 1:22 was chosen for each light-absorbing layer to generate a narrowband US signal. This resulted in 23.5% of the incident laser energy penetrating through the multilayer film for PA excitation. The waveform and spectrum of the US signal generated by this film are shown in Fig. 9. The US generated by the 10- μm thick single-layer film had a center frequency and fractional bandwidth of 24.2 MHz and 105.2%, respectively. While the center frequency of the US signal generated by the multilayer film was also 24.2 MHz, its fraction bandwidth was much lower at 26.8%, and the magnitude in

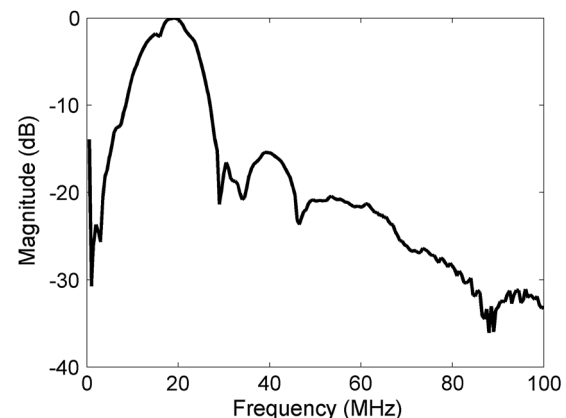


Fig. 11 The frequency response of the receiver transducer.

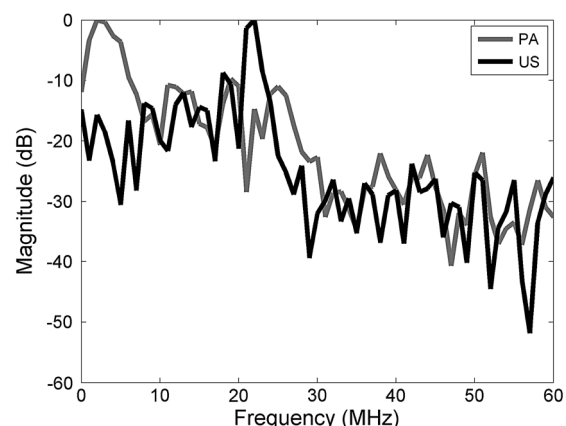


Fig. 12 Spectra of US and PA signals for the cyst-like phantom.

the frequency domain at frequencies below 17 MHz was less than -17 dB. This narrowband characteristic means that the US waves generated by this multilayer film can be used as a US source in US-PA imaging with single-laser pulses, and that the backscattered signals can be separated from low-frequency PA signals by simple spectral filtering.

US-PA images of the cyst-like phantom are shown in Fig. 10 and the frequency response of the receiving transducer is shown in Fig. 11. The total laser energy as measured by a laser power meter (Nova II, Ophir, Newton, Israel) with high-sensitivity thermal laser sensors (12A-P-SH, Ophir) for US and PA imaging was $17 \mu\text{J}/\text{pulse}$. The original image obtained before applying the filters is shown in Fig. 10(a). The US signals were extracted using a 19 to 25 MHz bandpass filter and a demodulation frequency of 22 MHz, while the PA signals were extracted using a 6 MHz lowpass filter and a demodulation frequency of 3 MHz. The sensitivity for the two bandwidths are -5.3 to 0 dB (for US imaging) and -30.7 to -13 dB (for PA imaging), respectively. The SAFT algorithm was applied after filtering. The PA and US images are shown in Figs. 10(b) and 10(c), respectively, while the fused US and PA images are shown in Fig. 10(d). The grayscale in the fused image shows the US image of the cyst-like phantom, where the pseudocolor (green) highlights the object with a high-optical absorption.

The filtering technique is effective in separating US and PA signals if there is a sufficiently large difference in the signal spectra between the multilayer film (US imaging) and the imaged object (PA imaging). Figure 12 shows the spectra of

the US and PA signals for the cyst-like phantom. Although the US signal generated by the multilayer film had a low magnitude below 20 MHz, the magnitude of the PA signal remained high around 20 MHz. This overlap in the spectra may affect the performance of this approach. This problem could be overcome by tuning the multilayer film to generate a higher-frequency narrowband US signal in order to further enhance the difference between the US and PA signals.

C-scan US-PA images of the thin-film phantom acquired by the all-optical scanhead [using the imaging setup shown in Fig. 7(b)] are shown in Fig. 13. The laser energies used in the US and PA imaging were 280 and 60 nJ/pulse, respectively. The maximum intensity projection results indicate that both the US backscattered from the thin plastic film and the PA signals generated by the carbon pattern were detected, with the US image showing the dark “US” pattern and the PA image showing the bright “PA” pattern [Fig. 13(a)]. Two bandpass filters were applied: the PA and US signals were enhanced by applying filtering from 9 to 11 MHz [Fig. 13(b)] and from 15 to 25 MHz [Fig. 13(c)], respectively. These two images were coregistered and are displayed as a fused image in Fig. 13(d).

4 Discussion

In general, a separate transducer can be used for generation of US for US-PA imaging. Nonetheless, in our approach, because a single-laser beam is used for generation of PA and US signals and a single transducer is used for detection, both PA imaging and US imaging are inherently coregistered. In addition,

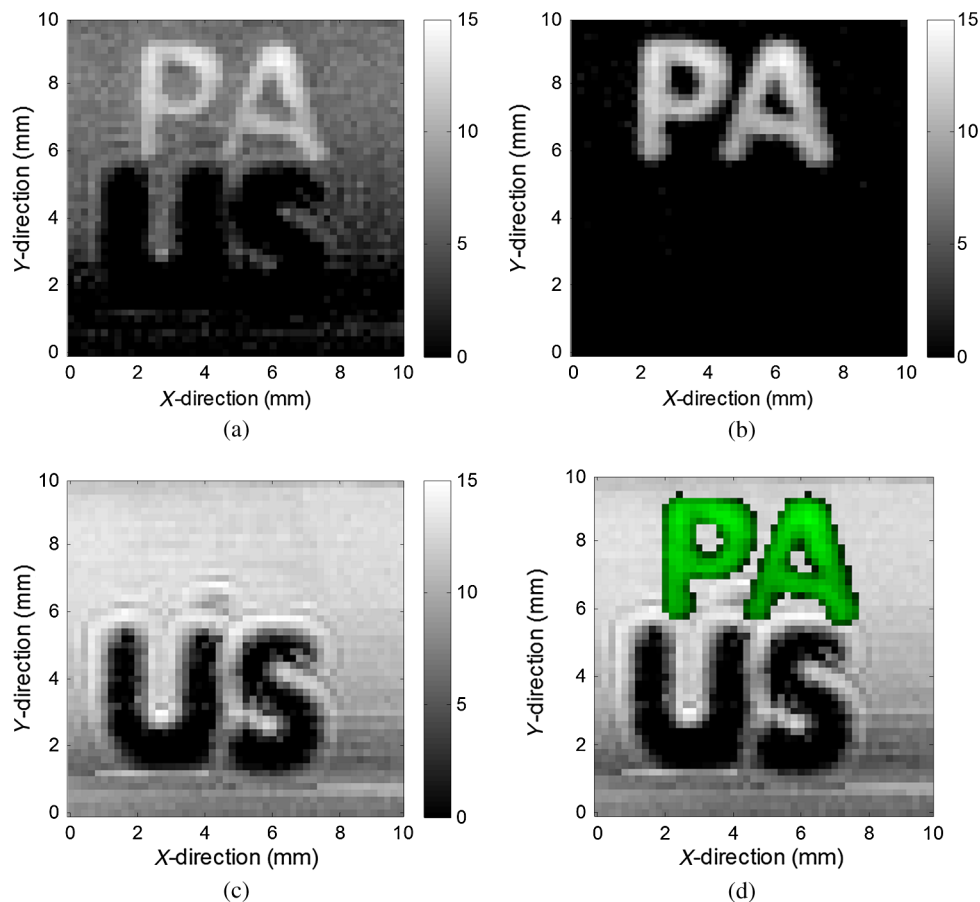


Fig. 13 (a) Image of the thin-film phantom obtained before filtering, and corresponding (b) PA, (c) US, and (d) fused images.

because only a multilayer film is needed for US generation, it is, in principle, a low-cost design compared to having a separate transducer for US imaging on transmission. This also makes it possible for the system to be miniaturized compared to the system requiring an additional US transmitter. On the other hand, our approach has the advantage of having a high-frame rate, which refers to the fact that at a single-laser pulse, both PA imaging and US imaging can be concurrently realized (i. e., without taking additional time for separate PA and US data acquisition).

The microring device used in one of the imaging setups in this study has several advantages, including being small (10 to 100 μm) and having a wide detection bandwidth (from DC to >90 MHz at -3 dB), adequate SNR (noise-equivalent pressure = 0.23 kPa over 1 to 75 MHz), and no requirement for complicated back-end circuitry.¹³ This kind of sensor can be integrated into a miniaturized transducer and its wide detection bandwidth is beneficial for detecting both US and PA signals. By combining the microring device with the single pulse approach proposed in this paper, the all-optical US-PA imaging transducer can be cost-effective, miniaturized, and have a high-imaging frame rate. In this design, the challenge is to integrate the multilayer film with the polymer microring resonator. A possible strategy is to fabricate the polymer microrings on a transparent substrate such as the glass substrate used in this study. Polymer microrings are fabricated using nanoimprint lithography, and can be fabricated on a transparent substrate such as SiO_2 .¹² In addition, the multilayer film can be fabricated at a lower temperature ($<100^\circ\text{C}$)¹⁵ than that used for polymer microring fabrication (180°C).¹⁶ Therefore, the multilayer film can be spun on the substrate of the microring resonator so that it is integrated into a miniaturized device for specific imaging applications.

5 Conclusions

This paper has demonstrated the application of a multilayer film for US and PA multimodality imaging. High-frequency US signals with a relatively narrow bandwidth can be optically generated by the multilayer film, which makes it possible to spectrally separate these signals from the low-frequency PA signals typically generated by biological tissue. The center frequency and fractional bandwidth of the US signals generated using the current setup were 24.2 MHz and 26.8%, respectively, and their magnitude below 17 MHz was less than -17 dB. These features can increase the difference between the US and PA signals. In addition, a single-laser pulse was employed to concurrently generate US on the multilayer film and generate PA signals from optical absorption by the imaged object. The imaging capabilities have been demonstrated using a cyst-like phantom and a thin-film phantom. The US and PA signals were effectively separated by filtering, and the imaging SNR was further improved by applying the SAFT. Multilayer films with different light-absorbing materials and production procedures could be explored to further increase the difference between the US and PA signals.

Acknowledgments

The authors would like to thank the reviewers for insightful comments. Financial supports from the Ministry of Science and Technology under grants 100-2221-E-002-146-MY3, 103-2811-8-002-001 and 102-2221-E-002-065-MY3 are gratefully acknowledged.

References

1. D. H. Turnbull et al., "A 40–100 MHz B-scan ultrasound backscatter microscope for skin imaging," *Ultrasound Med. Biol.* **21**(1), 79–88 (1995).
2. F. S. Foster et al., "Principles and applications of ultrasonic backscatter microscopy," *IEEE Trans. Ultrason. Ferroelectr. Freq. Contr.* **40**(5), 608–617 (1993).
3. S. Sethuraman et al., "Intravascular photoacoustic imaging using an IVUS imaging catheter," *IEEE Trans. Ultrason. Ferroelectr. Freq. Contr.* **54**(5), 978–986 (2007).
4. S. Y. Emelianov, P. C. Li, and M. O'Donnell, "Photoacoustics for molecular imaging and therapy," *Phys. Today* **62**(8), 34–39 (2009).
5. T. Buma, M. Spisar, and M. O'Donnell, "High-frequency ultrasound array element using thermoelastic expansion in an elastomeric film," *Appl. Phys. Lett.* **79**(4), 548–550 (2001).
6. Y. Hou et al., "Optical generation of high frequency ultrasound using two-dimensional gold nanostructure," *Appl. Phys. Lett.* **89**(9), 093901 (2006).
7. H. W. Baac et al., "Carbon-nanotube optoacoustic lens for focused ultrasound generation and high-precision targeted therapy," *Sci. Rep.* **2**, 989 (2012).
8. R. J. Colchester et al., "Laser-generated ultrasound with optical fibres using functionalised carbon nanotube composite coatings," *Appl. Phys. Lett.* **104**(17), 173502 (2014).
9. B. Y. Hsieh et al., "All-optical transducer for ultrasound and photoacoustic imaging by dichroic filtering," in *IEEE Int Ultrason Symp.*, pp. 1410–1413 (2012).
10. P. C. Li, C. W. Wei, and Y. L. Sheu, "Subband photoacoustic imaging for contrast improvement," *Opt. Express* **16**(25), 20215–20226 (2008).
11. C. Y. Chao et al., "High-frequency ultrasound sensors using polymer microring resonators," *IEEE Trans. Ultrason. Ferroelectr. Freq. Contr.* **54**(5), 957–965 (2007).
12. H. Li et al., "A transparent broadband ultrasonic detector based on an optical micro-ring resonator for photoacoustic microscopy," *Sci. Rep.* **4**, 4496 (2014).
13. Z. Deng et al., "Two-dimensional synthetic-aperture focusing technique in photoacoustic microscopy," *J. Appl. Phys.* **109**(10), 104701 (2011).
14. J. K. Tsou et al., "Role of ultrasonic shear rate estimation errors in assessing inflammatory response and vascular risk," *Ultrasound Med. Biol.* **34**(6), 963–972 (2008).
15. J. M. Cannata et al., "Development of a 35-MHz piezo-composite ultrasound array for medical imaging," *IEEE Trans. Ultrason. Ferroelectr. Freq. Contr.* **53**(1), 224–236 (2006).
16. S. W. Huang et al., "Low-noise wideband ultrasound detection using polymer microring resonators," *Appl. Phys. Lett.* **92**(19), 193509 (2008).

Shi-Yao Hung received his MS degree from the Graduate Institute of Biomedical Electronics and Bioinformatics at National Taiwan University in 2014. His main research interests include laser-generated ultrasound and photoacoustic imaging.

Wen-Shao Wu received his BS degree in electrical engineering from National Tsinghua University, Taiwan, in 2014. Currently, he is a master's student in biomedical electronics and bioinformatics at National Taiwan University. His research field is ultrasonic imaging and photoacoustic imaging.

Bao-Yu Hsieh received his MS degree from the Institute of Biophotonics at National Yang-Ming University, Taipei, Taiwan, in 2007, and his PhD from the Graduate Institute of Biomedical Electronics and Bioinformatics at National Taiwan University, Taipei, Taiwan, in 2012. Currently, he is a research senior fellow in the Department of Bioengineering, University of Washington, Seattle, USA. His current research interests include biomedical imaging and photoacoustic imaging.

Pai-Chi Li received his PhD from the University of Michigan in 1994. He joined Acuson Corporation as a member of the technical staff in June 1994. In August 1997, he went back to the Department of Electrical Engineering at National Taiwan University, where he is currently distinguished professor. He is also the TBF chair in biotechnology. His current research interests include biomedical ultrasound and medical devices.